Local adaptation under gene flow: Recombination, conditional neutrality and genetic trade-offs shape genomic patterns in *Arabidopsis lyrata*

Tuomas Hämälä[1,2,3] and Outi Savolainen[1,2,4]

[1]Department of Ecology and Genetics, University of Oulu, FI-90014 Oulu, Finland

[2]Biocenter Oulu, University of Oulu, FI-90014 Oulu, Finland

[3]E-mail: tuomas.hamala@gmail.com

[4]E-mail: outi.savolainen@oulu.fi

Abstract

Short-scale local adaptation is a complex process involving selection, migration and drift. The expected effects on the genome are well grounded in theory, but examining these on an empirical level has proven difficult, as it requires information about local selection, demographic history and recombination rate variation. Here, we use locally adapted and phenotypically differentiated *Arabidopsis lyrata* populations from two altitudinal gradients in Norway to test these expectations at the whole-genome level. Demography modelling indicated that populations within the gradients diverged less than 2 kya and that the sites are connected by gene flow. The gene flow estimates were, however, highly asymmetric with migration from high to low altitudes being several times more frequent than *vice versa*. To detect signatures of selection for local adaptation, we estimated patterns of lineage specific differentiation among these populations. Theory predicts that gene flow leads to concentration of adaptive loci in areas of low recombination; a pattern we observed in both lowland-alpine comparisons. Although most selected loci displayed patterns of conditional neutrality, we found indications of genetic trade-offs, with one locus particularly showing high divergence and signs of selection in both populations. Our results further suggest that resistance to solar radiation is an important adaptation to alpine environments, while vegetative growth and bacterial defense were indicated as selected traits in the lowland habitats. These results provide insights into genetic architectures and evolutionary processes driving local adaptation under gene flow. We also contribute to understanding of traits and biological processes underlying alpine adaptation in northern latitudes.

Introduction

Population genetics theory by Haldane (1930) and Wright (1931) laid the basis for predicting how selection and drift influence adaptive variation in the presence of gene flow. More recently, theoretical studies have shown that the interplay between these factors can lead to characteristic changes in genetic architectures underlying local adaptation (Griswold 2006; Yeaman and Whitlock 2011). An important prediction is the shift towards fewer large effect loci that are concentrated in areas of reduced recombination, as differences are more easily maintained in a set of correlated sites under strong selection (Slatkin 1975; Lenormand and Otto 2000; Griswold 2006). The adaptive loci are also expected to show antagonistic pleiotropy, wherein a single locus is kept polymorphic by differential selection to contrasting environments, because under the alternative scenario of conditional neutrality (allele has a fitness effect only in one environment, while being neutral in the other), the overall beneficial allele will be fixed at all populations over time (Yeaman and Whitlock 2011; Wadgymar et al. 2017; Yoder and Tiffin 2017). These effects can make the footprint of natural selection more distinct (Pfeifer et al. 2018; Wang et al. 2018), but migration also hinders adaptive divergence by swamping beneficial alleles (Lenormand 2002). Therefore, short-scale local adaptation is inevitably restricted to environments where spatially varying selection can overcome the homogenizing effects of the gene flow. For example, plant populations growing on toxic soils, either naturally occurring or contaminated by mine tailings, have exhibited such adaptation (Antonovics and Bradshaw 1970; Sambatti and Rice 2006; Arnold et al. 2016; Aeschbacher et al. 2017).

In the present study, we examine the genetic basis of local adaptation among lowland and alpine populations of a self-incompatible perennial plant, *Arabidopsis lyrata.* In mountainous environments, abiotic factors such as temperature and solar radiation can differ drastically among closely adjacent areas, producing steep environment gradients (Gonzalo-Turpin and Hazard 2009; Fischer et al. 2013; Kubota et al. 2015; Günther et al. 2016), not unlike those found on toxic soils. Indeed, we have recently demonstrated that *A. lyrata* individuals from different altitudes exhibited

population specific phenotypes when grown at native common garden sites in Norway and in a novel habitat in Finland (Hämälä et al. 2018). Using whole-genome based demography modelling and a reciprocal transplant experiment, we further showed that despite evidence of gene flow, local alpine and lowland populations had highest fitness at their home sites, satisfying the local vs. foreign criterion of local adaptation (Kawecki and Ebert 2004). This study system and the combined knowledge of local adaptation and demographic history, as well as genome-wide recombination information from a high density linkage map (Hämälä et al. 2017), provides us an rare opportunity to study genomic patterns of adaptive divergence under gene flow (Savolainen et al. 2013).

Here, we extend our previous work to the genome level by examining variation potentially underlying the local adaptation. If the alpine adaptation evolved after recent colonization from the lowland sites, the high-altitude populations are expected to show lower genetic diversities, higher accumulation of deleterious mutations, and stronger population size contractions than the low altitude populations. The ongoing gene flow then leads us to look for evidence of antagonistic pleiotropy (loci showing high differentiation and signs of selection in both populations) and loci kept polymorphic by reduced recombination. Furthermore, we expect to identify genes and biological processes underlying the lowland and alpine adaptation. We search for signs of selection by employing a measure for lineage specific differentiation, population branch statistic (PBS) (Yi et al. 2010), on a set of whole-genome sequences. Unlike traditional differentiation measures, PBS can distinguish the selected lineage by combining information from two closely related populations and an outgroup. As this method searches for allele frequency differences among populations, it is more likely to detect large effect loci instead of small effect ones underlying truly quantitative traits, because the latter signal may largely arise from linkage disequilibrium between populations (Latta 1998). We then explore the potential effects of selection with coalescent and forward simulations, utilizing parameter estimates available for these populations.

We specifically address the following questions: What do diversity patterns tell us about the demographic history of these populations, and do we find footprints of gene flow on this variation? Are there more selected sites in areas of reduced recombination in populations that receive more migrants? Is the genetic architecture dominated by conditional neutrality or do we find loci exhibiting variation consistent with antagonistic pleiotropy? And to what phenotypes and biological processes are the outliers associated with and do we find evidence of adaptive convergence between the two alpine areas?

Results

We used whole-genome data from 47 resequenced *A. lyrata* individuals. Most of the samples were collected from four populations growing in two alpine areas in Norway, each represented by a high and low group (Jotunheimen and Trollheimen): Lom, Jotunheimen (J1, 300 m.a.s.l.; n = 9), Spiterstulen, Jotunheimen (J3, 1,100 m.a.s.l; n = 12), Sunndalsøra, Trollheimen (T1, 10 m.a.s.l; n = 5) and Nedre Kamtjern, Trollheimen (T4, 1,360 m.a.s.l; n = 9). The abbreviations come from Hämälä et al. (2018). Based on patterns of microsatellite variation, populations within both alpine areas form distinct genetic clusters (Gaudeul et al. 2007). For some of the analysis, we also included samples from Germany (GER; n = 6) and Sweden (SWE; n = 6) as comparison groups. Data from the T4 population represent new collections for the current study, whereas other samples came from two earlier studies (Mattila et al. 2017; Hämälä et al. 2018).

Alpine populations harbour lower genetic diversities than lowland populations

Within each area, the high-altitude populations had lower synonymous nucleotide diversity estimates than the low-altitude populations ($p < 0.001$, Kolmogorov-Smirnov test [KST]) (Table 1). The high-altitude populations also had higher π_N/π_S ratios ($p < 0.001$, KST), likely indicating greater accumulation of deleterious mutations. Furthermore, synonymous Tajima's D estimates were more highly positive in the high-altitude populations ($p < 1\times10^{-16}$, KST), suggesting stronger population size contractions in their history. Differentiation levels, as estimated with F_{ST}, were lower between

the neighbouring lowland and alpine populations than between other comparison pairs (Table 1). The Jotunheimen populations were less differentiated from each other (J1-J3; $F_{ST} = 0.09$) than populations from Trollheimen (T1-T4; $F_{ST} = 0.17$).

Table 1. Location information and summary statistics for the study populations.

	Sampling location			Genetic diversity			Pairwise F_{ST}				
	Lat (N)	Lon (E)	Altitude (m.a.s.l)	π_S ($\times 10^{-3}$)	π_N/π_S	D	J1	J3	T1	T4	SWE
J1	61°84′	8°57′	300	7.20	0.261	0.49					
J3	61°62′	8°40′	1100	7.05	0.264	0.58	0.086				
T1	62°66′	8°62′	10	8.34	0.265	0.16	0.267	0.276			
T4	62°74′	9°30′	1360	7.01	0.268	0.49	0.305	0.312	0.165		
SWE	63°12′	18°57′	5	6.85	0.254	0.37	0.335	0.340	0.313	0.352	
GER	49°39′	11°29′	400	12.9	0.227	0.10	0.412	0.425	0.369	0.413	0.417

Synonymous nucleotide diversity (π_S), the ratio between nonsynonymous and synonymous diversity estimates (π_N/π_S) and synonymous Tajima's D (D) are median values estimated in 10 Kb non-overlapping windows. F_{ST} are weighted genome-wide averages estimated for synonymous sites.

We then conducted a principal component analysis (PCA) and an admixture analysis to further evaluate the relationships between the studied individuals. PCA showed distinct divisions, with individuals clustering according to populations and populations clustering according to geographical location (Fig. 1A). Consistent with the F_{ST} estimates, the Trollheimen populations were more clearly separated from each other than populations from Jotunheimen (Fig. 1B). In fact, in a model with only the focal populations included, variation along the first two principal components did not separate the J1 and J3 populations (separation happens at PC4; Fig. S1). The admixture patterns were in most part concordant with the PCA results. In general, individuals from the low-altitude populations J1 and T1 had higher admixture proportions (from their respective high-altitude neighbours) than individuals from the high-altitude populations J3 and T4 (from their low-altitude neighbours) (Fig. 1C).

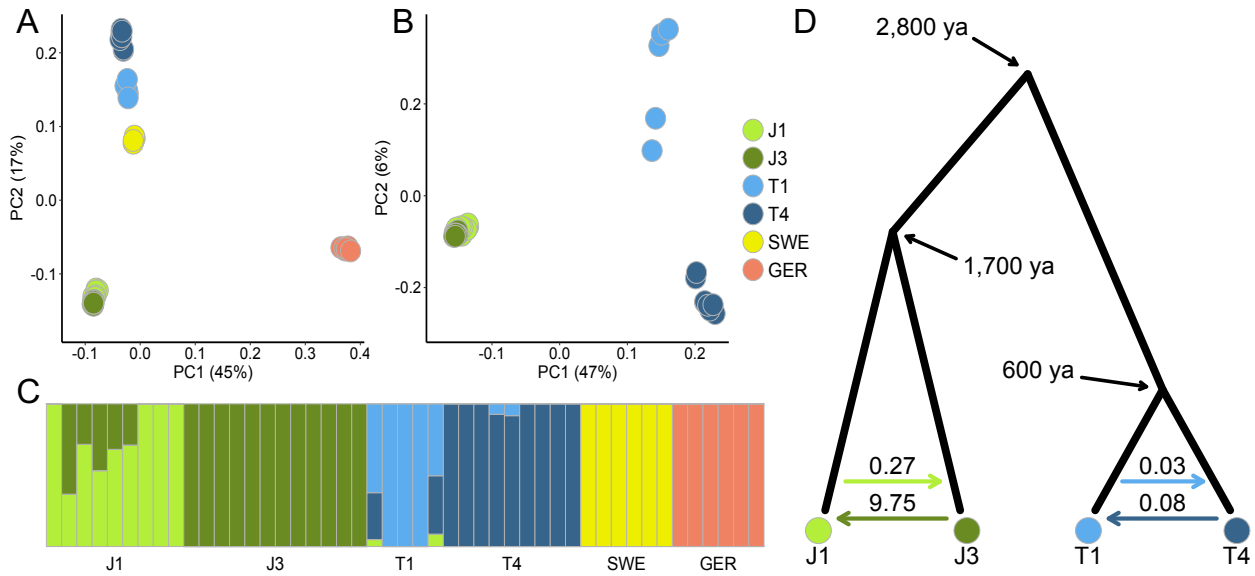

Figure 1. Visualization of the population structure and demographic history. Besides the Norwegian populations (J1, J3, T1, T4), individuals from Sweden (SWE) and Germany (GER) are included for comparison. **A:** Genetic variation along the first two eigenvectors of a principal component analysis (PCA). All six populations included. **B:** PCA with only the Norwegian populations included. The percentage of variance explained by the principal components are shown in brackets. **C:** Estimated admixture proportions when the number of ancestral populations is six. **D:** Estimated divergence times and migration rates between the Norwegian populations. Times are in years, while assuming a generation time of two years. Estimates above the coloured arrows indicate population migration rates ($4N_em$: number of migrant lineages per generation).

Demography analysis reveals recent divergence and asymmetric gene flow

To quantify the levels of gene flow, as well as to have an estimate of divergence times and effective population sizes, we conducted site frequency spectra based demography simulations in fastsimcoal2 (Excoffier et al. 2013). Simulations involving the Jotunheimen populations J1 and J3 were done as part of an earlier study (Hämälä et al. 2018) and here we add parameter estimates for the Trollheimen populations T1 and T4. Maximum likelihood estimates (MLE) from the best-supported models (for model selection, see Table S1) indicated more recent divergence between T1 and T4 (307 generations ago) populations then between J1 and J3 (866 generations ago) populations. The Trollheimen groups also had lower effective population size estimates (N_e: T1 = 1,862; T4 = 779) than the Jotunheimen groups (N_e: J1 = 3,370; J3 = 4,295). Although the levels of gene flow were clearly higher among the Jotunheimen populations, the population migration rates were heavily biased towards the low altitude populations in both alpine areas (~36× higher from J3 to J1 than from J1 to J3, and ~2.4× higher from

T4 to T1 than from T1 to T4) (Fig. 1D). As *A. lyrata* is insect pollinated, the asymmetry in gene flow could result from higher seed dispersal from high- to low-altitudes, but because allele frequencies reflect events over extended periods of time, we cannot rule out other modes of migration that may have been in effect during colonization of the alpine areas. For all MLEs and their 95% confidence intervals, see Table S2.

Genome-wide patterns of population specific selection

We studied population specific differentiation to examine the effects of gene flow on neutral and selected variants and to ascertain the important biological processes at each lowland and alpine habitat. To this end, we used population branch statistic (PBS) (Yi et al. 2010) to distinguish loci that have been under directional selection after the adjacent low- and high-altitude populations diverged. We first applied a maximum likelihood model by Kim et al. (2011) to estimate allele frequencies for each population directly from the genotype likelihoods. This method bypasses the need for genotype calling, leading to unbiased allele frequency estimates even at low coverage. The pairwise differentiation estimates between three populations, two focal ones and an outgroup, were quantified using a relative measure, F_{ST}, and an absolute measure, d_{XY}. As these measures can be inflated by reduced within population genetic diversities and unequal sample sizes, respectively, we focused on outliers that were confirmed by both measures. For outlier detection, we used a method based on simulated null distributions. Estimated demography parameters (divergence times, migration rates and effective population sizes, going back to most recent common ancestor) and recombination information from a linkage map (Hämälä et al. 2017) were used to model the expected neutral differentiation statistics for these populations.

Selection patterns between the neighbouring populations were examined by calculating PBS estimates in 50 SNP non-overlapping sliding windows for population trios J1-J3-GER and T1-T4-GER. The German population was chosen as the outgroup over the Swedish one, because it has a more equal genetic distance to each of our focal populations (Fig. 1A and Table 1). Using the

simulated neutral data, we first generated ~50,000 PBS samples for each population and used the distributions to find limits to neutral variation in the observed data. The simulations predicted lower median estimates and more tightly centred distributions in the low-altitude populations (median: J1 = –0.007, T1 = –0.009; IQR: J1 = 0.050, T1 = 0.078) than in the high-altitude populations (median: J3 = –0.006, T4 = 0.002; IQR: J3 = 0.053, T4 = 0.081). Overall, the observed estimates corresponded well with the simulated data. Within both areas, the low-altitude populations had lower median estimates than the high-altitude populations (J1 = –0.009, J3 = –0.004, T1 = –0.017, T4 = 0.007) and the distributions were less dispersed around the median (IQR: J1 = 0.060, J3 = 0.063, T1 = 0.093, T4 = 0.108). The observed distributions did, however, have slightly longer lower and upper tails than the neutral ones (Fig. S2), indicating possible balancing and directional selection, respectively. Significant deviations from the neutral expectations were determined by defining *p*-values for the observed estimates through comparisons against quantiles of the simulated distributions. The *p*-values were subsequently transformed into false discovery rate based *q*-values to reduce the bias caused by multiple testing. PBS estimates with *q*-value less than 0.05 were considered as significant. Our outlier detection model predicted fewer selected loci in the low-altitude populations than in the high-altitude populations (bracketed values indicate percentages of the total data sets): J1 = 896 (1.1%), J3 = 948 (1.2%), T1 = 966 (1.3%) and T4 = 1,160 (1.6%) (Fig. S3). Although all outlier windows tended to localize in areas with lower than average per base pair recombination rates (genome-wide average = 3.7×10^{-8}), this trend was more pronounced in the low-altitude populations (median estimates with 50 SNP sliding windows): J1 = 2.13×10^{-8}, J3 = 2.72×10^{-8}, T1 = 2.37×10^{-8} and T4 = 2.56×10^{-8} ($p < 0.003$, KST). The same pattern also persisted with longer window sizes (150 SNP window): J1 = 2.10×10^{-8}, J3 = 2.54×10^{-8}, T1 = 2.14×10^{-8} and T4 = 2.8×10^{-8} (*p*-value < 0.009, KST).

Evidence of allelic trade-off at *XRN2* locus

Most selection outliers were found only in a single population (Table S3), likely indicating conditional neutrality. Some loci were, however, shared between the neighboring low- and high-altitude populations, suggesting possible antagonistic pleiotropy: 42 out of 1,668 genes that were found within 5 Kb of an outlier window were shared between J1 and J3 (based on 10,000 randomized data sets [randomization test from now on], the expected number of shared outliers is 22), while 67 out of 2,359 were shared between T1 and T4 (43 expected, randomization test). One locus (*XRN2*) particularly stood out as one of the top outliers in T1 and T4, caused by higher than neutral differentiation between all three population comparisons (i.e. T1-T4, T1-GER and T4-GER). To examine whether the observed pattern might result from directional selection favoring different alleles in different populations (antagonistic pleiotropy), we examined allele frequencies, as well as pairwise nucleotide diversities (π) and Tajima's *D* estimates around the gene. Reduced diversity surrounding the selected site is a classical signal of a rapid selective sweep, whereas Tajima's *D* detects skews in the site frequency spectrum, producing negative estimates when the number of rare alleles exceeds neutral expectations; a pattern also consistent with a selective sweep. Allele frequencies showed clear evidence of differentiation, with T1 fixed for one allele and T4 nearly fixed for the alternative allele. Both populations also had reduced nucleotide diversities and negative Tajima's *D* estimates in ~8 Kb area around the gene, indicating directional selection in each lineage (Fig. 2). To evaluate the likelihood of the observed patterns under our estimated demography parameters (Fig. 1D), we used forward genetic models in SLiM 2 (Haller and Messer 2017) to simulate nucleotide diversities and Tajima's *D* estimates under different selection scenarios. The recombination rate (3.7×10^{-8}) was obtained from the corresponding area of the linkage map. For the purpose of these simulations, we assumed constant population sizes so as not to confound the selection patterns with genetic bottlenecks. Like selection, a bottleneck can reduce genetic diversity, but given the highly localized nature of our findings (Fig. 2), it is an unlikely source for the observed

patterns. We ran the simulation $10\times N_e$ generations to approach mutation-drift balance, introduced the sweep mutation with selection coefficient α ($2N_es$) = 10^2, 10^3 and 10^4, and recorded the time in number of generations until π and D dropped below the initial neutral estimate. The simulations were conducted as single-origin hard sweeps and as multiple-origin soft sweeps. For the soft-sweeps, we assumed that 5% of the corresponding population carried the adaptive allele before the selection shift. Each simulation was repeated 300 times and the median value retained. Our models showed that under a hard sweep with strong selection ($\alpha > 10^3$), π and D can respond to selection in both populations within the estimated time frame (faster in T4 as it had lower N_e estimate [Fig. S4]). The same, however, was not true for lower selection coefficients or multiple-origin soft sweeps in general (Fig. 3).

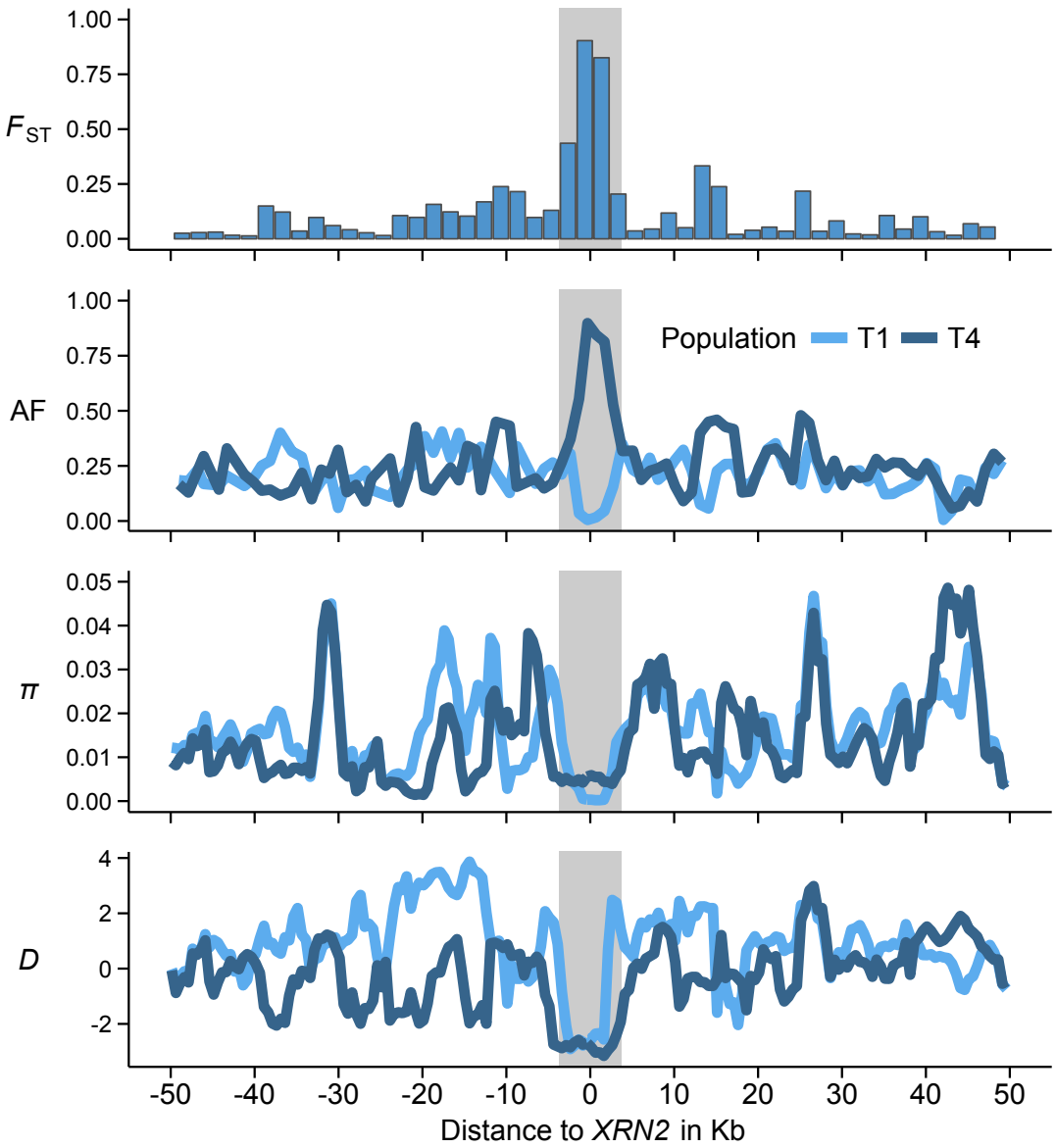

Figure 2. Evidence of opposing selective sweeps between T1 and T4 populations at candidate loci *XRN2* (shaded area). F_{ST} gives the relative differentiation proportions. AF shows frequencies of the non-reference SNP alleles. Nucleotide diversity π and Tajima's D indicate a loss of heterozygosity and an excess of rare variants, respectively.

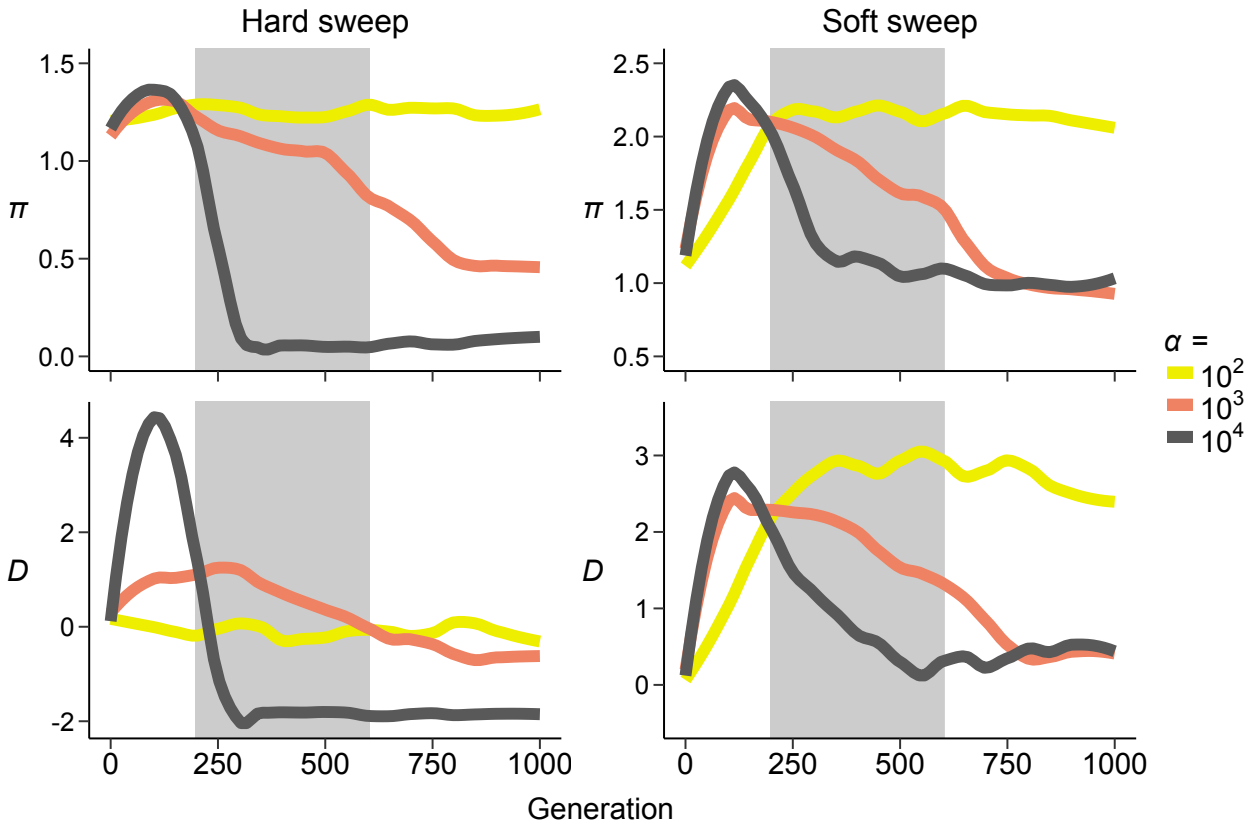

Figure 3. Nucleotide diversity π ($\times 10^{-3}$) and Tajima's D estimates simulated for 8 Kb area. The simulations were ran as single-origin hard sweeps and as multiple-origin soft sweeps. For the latter case, we assumed an initial frequency of 0.05 for the adaptive allele. Shown are median estimates from 300 simulations. Shaded area marks the 95% confidence intervals for the estimated divergence time between T1 and T4 populations. Parameters: $2N_e$ = 3,724 (corresponding to T1 estimate), α ($2N_es$) = 10^2, 10^3, 10^4, $\mu = 7\times10^{-9}$ and $r = 3.7\times10^{-8}$. For T4 population, see Fig. S2.

Biological processes show adaptive convergence

Most genes that localized within 5 Kb of the outlier windows were population specific (Table S3). Among the significant outlier loci, 49 out of 1,785 genes were shared between the two low-altitude populations (25 expected, randomization test), whereas in the high-altitude populations, 92 genes were shared out of 2,240 (38 expected, randomization test). We then conducted a Gene Ontology (GO) enrichment analysis to summarize the biological processes associated with our outlier genes. In contrast to individual loci, significantly enriched GO terms showed clear correlations among the low- and high-altitude populations (Fig. 4). In the J1 and T1 populations, 'leaf development', 'shoot system development' and 'response to bacterium' were among the highest enriched GO categories, whereas

the J3 and T4 outliers were enriched for terms ‘response to radiation’, ‘response to light stimulus’ and ‘cellular response to stress’.

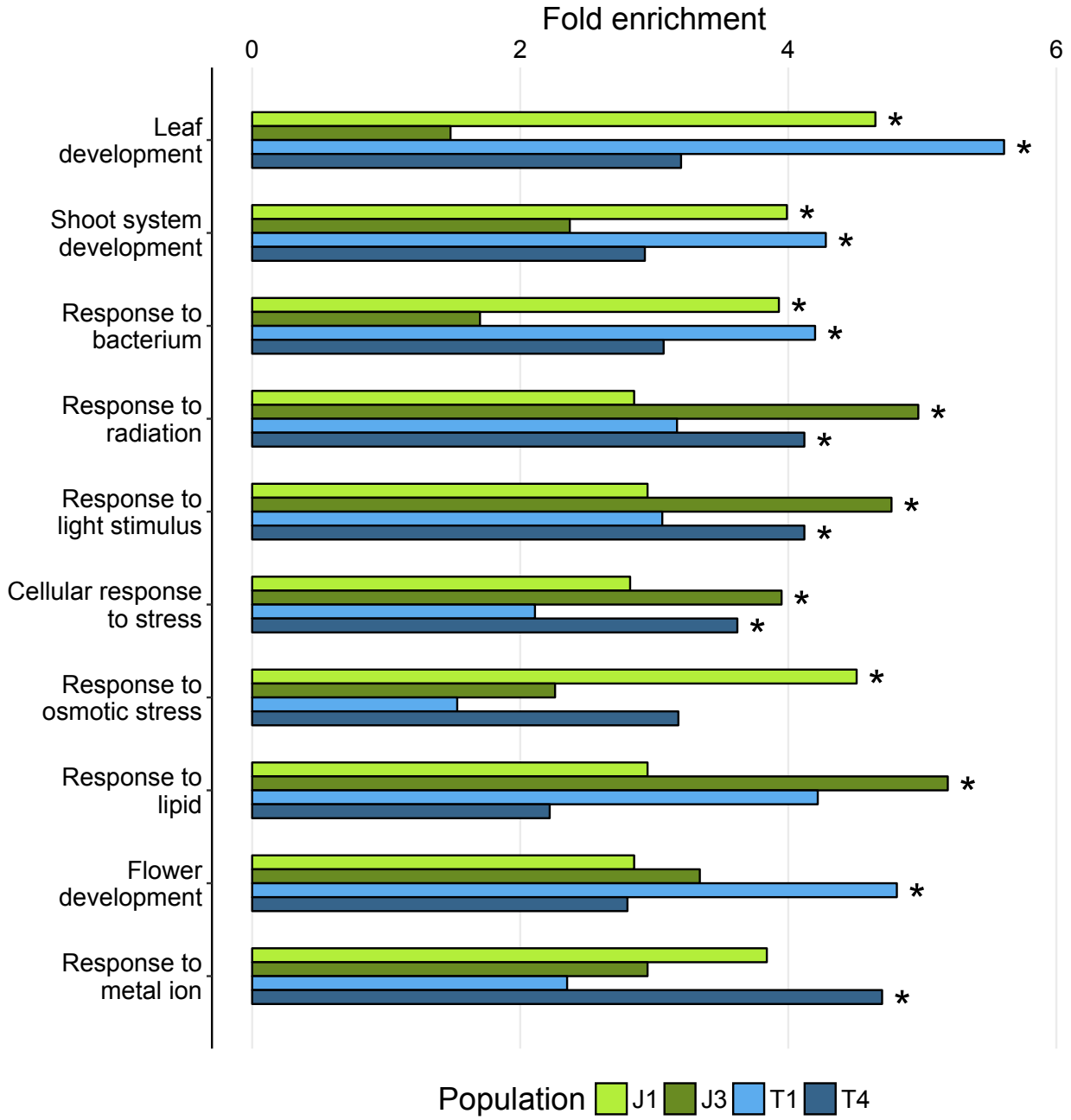

Figure 4. Highest enriched shared and unique GO terms with more than ten supporting genes among the significant ($q < 0.05$) PBS outliers. Terms with Bonferroni corrected p-value < 0.05 are marked with a star.

Discussion

We found indications of lower genetic diversities, higher accumulation of deleterious mutations and stronger population size contractions in the high-altitude populations than in the low-altitude populations. Combined with the low divergence time estimates from the demography models, these results point towards recent colonization of the alpine habitats in southwestern Norway. In contrast, highland populations in regions not influenced by the last glacial maximum (~20,000 years ago). likely reflect adaptation on a longer time scales [e.g. *A. halleri* in Japan (Kubota et al. 2015) and *A. thaliana* in Italy (Günther et al. 2016)], making our *A. lyrata* population set particularly suitable system for studying recent adaptation among populations connected by gene flow.

Gene flow shapes patterns of neutral and adaptive variation

The effects of gene flow on genetic patterns of local adaptation have been intensely studied at the theoretical level (Lenormand and Otto 2000; Griswold 2006; Yeaman and Whitlock 2011; Aeschbacher et al. 2017), but the empirical support for number of key predictions are still weak or missing. For example, under higher levels of gene flow, is adaptation attributable to fewer large effect loci that are concentrated in areas of reduced recombination? The use of PBS allowed us to approach these questions by examining the lineage specific differentiation patterns among populations that receive variable number of migrants. The demography modelling indicated ongoing, but highly asymmetric, gene flow between the neighbouring low- and high-altitude populations, while the Jotunheimen groups J1 and J3 exchanged migrants at a significantly higher rate than the Trollheimen groups T1 and T4. Concordant with these estimates, the low-altitude populations T1 and J1 showed PBS distributions with lower and less dispersed overall estimates than the high-altitude populations J3 and T4, and our simulation based outlier detection model predicted more adaptive loci in the high-altitude populations. Our results also showed that outlier windows in the low-altitude populations were more concentrated in areas of lower recombination rates than in the high-altitude populations. Similar patterns have previously been found among stickleback population pairs that presumably

exchange migrants at different rates (Marques et al. 2016; Samuk et al. 2017). However, by combining estimates of bidirectional gene flow with lineage specific selection analysis, we were able to examine these patterns not only between the Jotunheimen and Trollheimen study pairs, but also within them, making it possible to ascertain asymmetric effects and to better approach the genetic architecture underlying the local adaptation. Furthermore, despite a conscious effort (Renaut et al. 2013), significant associations between gene flow and recombination induced localization of the adaptive loci has not (to our knowledge) previously been reported in any other plant taxa. Based on theory, if the genetic architecture underlying local adaptation with gene flow evolves only through *de novo* mutations, a considerable amount of time may be needed for the signature patterns to form (Yeaman and Whitlock 2011). As the observed recombination differences have evolved recently, potentially during the last 1,000 generations, favourable patterns were likely present as standing genetic variation before the selection shift, leading to faster evolution of the genetic architecture.

Selection patterns indicate antagonistic pleiotropy between neighbouring populations

A major question in local adaptation research concerns the role of antagonistic pleiotropy in promoting adaptive divergence (Kawecki and Ebert 2004; Savolainen et al. 2013; Tiffin and Ross-Ibarra 2014; Wadgymar et al. 2017; Yoder and Tiffin 2017), and this issue is particularly relevant when the focus is on closely adjacent populations (Yeaman and Whitlock 2011). A traditional way to search for genetic trade-offs is to measure presumably adaptive trait variation in contrasting environments and to find correlations between phenotypes and genotypes through genetic mapping (Fournier-Level et al. 2011; Anderson et al. 2013; Ågren et al. 2013). Although this approach has the potential advantage of linking phenotypes to fitness, focusing on preselected traits might cause important factors to be overlooked. Furthermore, the causative genes underlying the often-wide quantitative trait loci (QTL) intervals have rarely been discovered. Here, we used PBS scans to find loci showing patterns of opposing selection among the neighbouring low- and high-altitude

populations, because under gene flow and unrestricted recombination, the frequency differentiation can only be maintained by such fitness trade-offs.

Our analysis discovered one locus (*XRN2*) with clear evidence of allelic trade-off between the T1 and T4 populations. In *A. thaliana*, *XRN2* is known to be involved in various RNA processing tasks (Zakrzewska-Placzek et al. 2010), including posttranscriptional gene silencing (Gy et al. 2007); a defence response against viral mRNAs. Examination of nucleotide diversities and Tajima's *D* estimates showed that the observed sequence patterns have likely resulted from two rapid and opposing selective sweeps, while the forward simulations indicated that selection has to be strong to produce these patterns in just under 600 generations (the upper confidence interval for the divergence time estimate). Furthermore, as suggested by our simulations, the highly negative Tajima's *D* estimates are likely the result of a single or very few haplotypes being swept to a high frequency in each population. The sweeps might, however, have started from a standing genetic variation, but due to low N_e and high drift, nearly all haplotypes were lost during the initial selection phase, producing hard sweep like patterns (Hermisson and Pennings 2017). Reduced recombination is not a likely factor here, because our linkage map, as well as the relatively short area affected by the selective sweeps (~8 Kb), indicates that the recombination rate in this area is close to genome-wide average. However, projected against the theory of selection-migration balance (Lenormand 2002), the near-fixation of alleles at this locus is likely facilitated not only by strong selection, but also by weak migration. Indeed, some loci were also found as outliers in both Jotunheimen populations, which are connected by stronger gene flow, but none exhibited the same extreme patterns of selective sweeps as *XRN2* in the Trollheimen populations. Based on expectations of mutational effects, conditional neutrality may actually be the dominant driver of local adaptation across all environments, as it can evolve through purely deleterious mutations (as opposed to antagonistic pleiotropy, which requires a beneficial effect in at least one environment) (Martin and Lenormand 2006). The method used here, however, searches for signals of positive selection, so the observed patterns are likely

influenced by the lack of power to distinguish selection in both lineages, leading to some trade-off loci being identified as conditionally neutral (Wadgymar et al. 2017; Yoder and Tiffin 2017). The divergence between these populations might also be too recent for antagonistic pleiotropy to become more common, as it is a prediction based on longer evolutionary time scales (Yeaman and Whitlock 2011). Although QTL mapping based studies have suggested that genetic trade-offs may be more frequent between the long since diverged Swedish and Italian *A. thaliana* populations (Ågren et al. 2013; Price et al. 2018), the absence of gene flow makes comparisons to our results problematic. In any case, the apparent prevalence of conditional neutrality can result in freer spread of alleles, which might be beneficial for these *A. lyrata* populations upon climate change (Fournier-Level et al. 2011; Hämälä et al. 2018). Furthermore, the discovery of a strong allelic trade-off at *XRN2* locus and the evaluation of the underlying processes requires detailed information about local selection, demographic history and recombination rate variation, which has rarely been available for other study systems.

Resistance to solar radiation is selected for in alpine environments

Besides genome-wide patterns of adaptive divergence, our results revealed genes and biological process that may underlie colonization of alpine and lowland habitats in southwestern Norway. A major factor associated with highland environments is the increase in solar radiation intensity (Körner 2007). Indeed, earlier study on *A. halleri* in Switzerland (Fischer et al. 2013) detected signs of directional selection on UV resistance genes in high-altitude populations. Our analysis also discovered a UV resistance gene *TT5* (Li et al. 1993) among the most significant outliers in J3 and a DNA break repair (a trait related to increased radiation levels) gene *RAD23C* (Farmer et al. 2010) was found in T4. Furthermore, genes involved in response to light stimulus were discovered in both populations, and the highest shared outlier between J3 and T4 was *ADG1*; a gene thought to be important in acclimation to high light intensities in *A. thaliana* (Schmitz et al. 2014). As indicated by our GO enrichment analysis, loci involved in 'response to radiation' were more numerous than

expected among the outlier loci in the two alpine populations. Additional highly enriched GO categories were 'response to light stimulus' and 'cellular response to stress', which might also be linked to adaptation under increased solar radiation ('response to high light intensity' was also significantly enriched in T4). The selection on radiation resistance genes may not, however, be ubiquitous among highland populations, as shown by studies on *A. halleri* in Japan (Kubota et al. 2015) and on *A. thaliana* in Italy (Günther et al. 2016). Therefore, these results indicate that solar radiation imposed selection can be a significant driver of adaptive divergence in the northern latitudes, even though the high-altitude areas in Scandinavia are relatively low elevation when compared to highest regions in the world.

Vegetative growth and bacterial defence are important traits in lowland adaptation

We also discovered interesting selection patterns in the low-altitude populations. Genes involved in leaf development and vegetative growth were found among the top outliers in J1 and T1, and the corresponding 'leaf development' GO category was significantly enriched in both gene sets. 'Shoot system development', another significantly enriched term, is especially interesting, because we have previously shown that lowland populations generally produce longer flowering shoots than alpine populations, and the trait had a positive correlation with fitness at the Finnish sea level field site (Hämälä et al. 2018). Bacterial defence seems to be another important trait in the lowland habitats. The GO term 'response to bacterium' was significantly enriched in both lowland populations, and the top outlier in J1 (*SRT2*) is involved in that process (Wang et al. 2010). Selection on bacterial defence genes has previously been discovered among populations from different altitudes in *A. halleri* (Fischer et al. 2013; Kubota et al. 2015) and in *A. thaliana* (Günther et al. 2016), but as those studies relied on traditional divergence outlier methods, the authors could not infer whether the selection target had been the low- or the high-altitude lineage. Furthermore, *XRN2*, the gene exhibiting allelic trade-off between T1 and T4, is thought to be involved in immune responses in *A. thaliana* (Gy et al.

2007), but it also has a role in general RNA processing (Zakrzewska-Placzek et al. 2010), so the causal factor behind the trade-off may not be related to pathogen defence.

Despite the fact that many genes with same biological processes were shared between the two high- and low-altitude populations, almost all individual loci were population specific, and none of the most significant ones have previously been found in altitude related genome scans in other *Arabidopsis* species (Fischer et al. 2013; Kubota et al. 2015; Günther et al. 2016). This lack of correlation at the gene level likely indicates that populations (and related species) living in similar environments have responded to same environmental pressures through different genetic pathways, suggesting either subtle differences in phenotypes under selection or that selection has acted on different genes underlying the same polygenic traits. Considering the recent divergence time estimate between populations from the two alpine areas (~2,400 years ago) and the growing evidence of convergent local adaptation even among more distantly related groups (Hohenlohe et al. 2010; Arnold et al. 2016; Yeaman et al. 2016), these results indicate that adaptation to altitude specific environments in *A. lyrata* is not constrained to only few key genes, which might further aid adaptation to future climates.

Conclusions

By studying recently diverged, phenotypically differentiated and locally adapted *A. lyrata* populations, we have gained novel insights into the adaptive processes driving differentiation under ongoing gene flow. Our approach of combining estimates of bidirectional gene flow with lineage specific selection analysis allowed us to examine population differences in genetic architectures underlying the local adaptation and to infer how asymmetric gene flow affects these patterns. The overall levels of gene flow were heavily biased towards the low-altitude populations, with J1 and T1 receiving several times more migrants than J3 and T4. As predicted by theory, the lowland populations had more selection outliers in areas of reduced recombination rates than the alpine populations. Furthermore, we found a locus showing clear footprints of strong opposing selective

sweeps in the Trollheimen populations; a pattern likely caused by antagonistic pleiotropy. However, most selected loci showed indications of conditional neutrality, potentially reflecting the recent divergence between these populations. Phenotypes associated with the outlier loci also revealed biological processes that may underlie alpine and lowland adaptation in northern Europe. Resistance to increased levels of solar radiation is likely an important factor for alpine populations, while in the lowland habitats, selected genes were involved in vegetative growth and bacterial defence. These results contribute to understanding of processes driving adaptive differentiation under gene flow, as well as of traits and biological processes underlying alpine adaptation in northern latitudes.

Materials and methods

Study populations

We studied altitude adaptation among Norwegian *A. lyrata* populations from two alpine areas (Jotunheimen and Trollheimen). Both areas were represented by one low- and one high-altitude population. The fitness and phenotypic variation of these populations were previously studied in Hämälä et al. (2018). In that study, the areas were represented by four populations, which were abbreviated as J1 to J4 and T1 to T4. Here, we retain the naming convention and call the populations J1 (300 m.a.s.l), J3 (1,100 m.a.s.l), T1 (10 m.a.s.l) and T4 (1,360 m.a.s.l). The distance between the J1 and J3 growing sites is approximately 25 km, whereas the approximate distance between T1 and T4 is 30 km. The two alpine areas are roughly 100 km apart. We previously showed that individuals from J1 and J3 exhibited local superiority when grown at reciprocal common garden sites in Norway. The T1 and T4 individuals were not planted at their local environments, but when grown at common garden in Finland, they expressed phenotypic differences consistent with altitude adaptation (Hämälä et al. 2018).

Whole-genome sequencing

Whole-genome data from two previously published studies were used (Mattila et al. 2017; Hämälä et al. 2018) nine individuals from J1, 12 from J3 and five from T1. For the present study, we also

resequenced nine individuals from T4 population, which exhibited more high-altitude specific phenotypes (earlier flowering start and shorter flowering shoots) in our field experiments than the previously sequenced T3 population (Hämälä et al. 2018). In addition, a German population (abbreviated as GER) consisting of six individuals was used as an outgroup in the selection scan (see 'Selection scan' -section) and the German and a Swedish population (SWE; consisting also of six individuals) were used as comparison groups in admixture and principal component analysis (see 'Analysis of genetic diversity and population structure' -section). The German and Swedish individuals, as well as five individuals from J3, came from Mattila et al. (2017), whereas the other previously sequenced individuals were from Hämälä et al. (2018). In all three studies, DNA was extracted from fresh leaves using NucleoSpin Plant II kits (Macherey-Nagel), the libraries for Illumina whole-genome sequencing were prepared with NEBNext master mix kits (New England Biolabs) and the sequencing was done with Illumina HiSeq2000 (Mattila et al. 2017) and HiSeq2500 (Hämälä et al. 2018; this study) in Institute of Molecular Medicine Finland, University of Helsinki, using PE100 chemistry. The median read coverage per individual ranged from six to 25. The low coverage in some individuals combined with the variable nature of the short-read sequencing means that information contained in large part of the data set is insufficient to call genotypes with high confidence (Nielsen et al. 2011). Therefore, to lessen the bias caused by uncertain genotypes, we adopted a SNP call free approach and based all estimated statistics on genotype likelihoods.

Sequence processing and allele frequency estimation

Low quality reads and sequencing adapters were removed using Trimmomatic (Bolger et al. 2014). The reads were aligned to *A. lyrata* v1.0 reference genome (Hu et al. 2011) with bwa-mem (Li and Durbin 2009). Duplicated reads were removed with Picard tools (https://broadinstitute.github.io/picard/) and indels realigned with GATK (DePristo et al. 2011). Likelihoods for the three possible genotypes in each biallelic site were then calculated with the GATK model in ANGSD (Korneliussen et al. 2014). We only used reads with mapping quality over 30,

while sites needed to have quality over 20 and sequencing depth no less than 4×. Allele frequencies for the selection scan were then estimated directly from the genotype likelihoods using a maximum likelihood model by Kim et al. (2011). The strict filtering associated with SNP calling (commonly the ranking genotype needs to be ten times more likely than the others) can especially reduce the number of heterozygote calls in areas of low coverage (for a comparison between SNP calls and genotype likelihoods in our data, see Figure S2). The method used here circumvents that problem by taking the genotype uncertainty into account, producing unbiased allele frequency estimates even with the minimum threshold coverage (Kim et al. 2011; Nielsen et al. 2011).

Analysis of genetic diversity and population structure

We studied genetic variation within populations by estimating three summary statistics with ANGSD (Korneliussen et al. 2014): nucleotide diversity π (Nei and Li 1979); the ratio of nonsynonymous and synonymous pairwise differences (π_N/π_S; estimated for 0-fold and 4-fold sites, respectively), which can estimate the efficacy of selection and the accumulation of deleterious mutations (e.g. Chen et al. 2017); and Tajima's *D*, which approximates how far the population is from a mutation-drift balance (Tajima 1989). Admixture analysis and principal component analysis (PCA) were conducted to further assess the genetic relationships between the study populations. ANGSD was used to estimate genetic covariance's for the PCA and genotype likelihoods for the admixture analysis (both estimated for 4-fold sites). The latter was conducted with NGSadmix (Skotte et al. 2013), by estimating admixture proportions for each individual from the genotype likelihoods.

Demography simulations

Site frequency spectra based coalescent simulations were used to estimate divergence times, migration rates and effective population sizes. Estimates involving the Jotunheimen populations J1 and J3 were inferred as part of an earlier study (Hämälä et al. 2018). Here, we conducted additional simulations for the Trollheimen populations T1 and T4 using the same method as in the earlier study. Briefly, derived site frequency spectra were estimated for 4-fold degenerate sites in ANGSD

(Korneliussen et al. 2014) and the demography models were fitted to these in fastsimcoal2 (Excoffier et al. 2013). We tested four different migration models between the Norwegian populations: no migration, unidirectional migration (from 1 to 2 and from 2 to 1) and bidirectional migration. Simulation were repeated 50 times to acquire global maximum likelihood estimates for the parameters. Model selection was based on Akaike information criterion (AIC) scores. We then used 100 nonparametric bootstrap site frequency spectra to define 95% confidence intervals for the parameter estimates. For more information about the demography analysis, see Hämälä et al. (2018).

Selection scan

Selected sites were detected by scanning the chromosomes for areas of unexpectedly high differentiation between the populations; a pattern indicative of directional selection (Lewontin and Krakauer 1973). The relative levels of differentiation were estimated with F_{ST} measure by Hudson et al. (1992): $1 - (H_W / H_B)$, where H_W and H_B are the mean number of differences within and between populations, respectively. However, here we used a more specific formula, developed for the two population, two allele case by Bhatia et al. (2013):

$$F_{\mathrm{ST}} = \frac{(p_1 - p_2)^2 - \frac{p_1(1-p_1)}{n_1 - 1} - \frac{p_2(1-p_2)}{n_2 - 1}}{p_1(1-p_2) + p_2(1-p_1)}$$

where n_i is the sample size and p_i is the minor allele frequency in the two populations to be compared. This estimator has been shown to be unbiased by unequal sample sizes and less prone to overestimating differentiation than measures by Weir and Cockerham (1984) or Nei (1986) (Bhatia et al. 2013). The selection scan was conducted in 50 SNP non-overlapping sliding windows (median length ~2 Kb), to prevent biasing the estimates with unequal SNP numbers. F_{ST} for a window of size n was calculated using the weighting method by Reynolds et al. (1983): $1 - (\sum_{i=1}^{n} H_{iW} / \sum_{i=1}^{n} H_{iB})$. For lower number of markers (such as within windows), this approach is often more reliable than averaging the F_{ST} estimates over loci (Weir and Cockerham 1984; Weir and Hill 2002; Bhatia et al. 2013). F_{ST} can, however, be inflated by reduced within-population nucleotide diversities, brought on

e.g. by background selection or impaired recombination (Charlesworth 1998; Cruickshank and Hahn 2014). For this reason, we also estimated absolute levels of differentiation between the populations; an index commonly called d_{XY} (Nei 1987; Cruickshank and Hahn 2014). To make it compatible with allele frequencies estimated from genotype likelihoods, d_{XY} for a window of size n was calculated by simply excluding the within-populations component of F_{ST}:

$$d_{XY} = \frac{1}{n}\sum_{i=1}^{n} p_{i1}(1 - p_{i2}) + p_{i2}(1 - p_{i1})$$

This measure is indifferent to within-population levels of diversity, but it can be biased by unequal sample sizes. Therefore, to balance the shortcomings of both F_{ST} and d_{XY}, we only considered sites that were detected as outliers using both measures.

A single differentiation measure, either F_{ST} or d_{XY}, can detect localized selection, but it cannot distinguish which lineage has been the target. A recently developed method, PBS (Yi et al. 2010), overcomes this limitation by comparing differentiation estimates between two closely related populations and an outgroup. The F_{ST} and d_{XY} values were first transformed into relative divergence times: $T = -\ln(1 - X)$, where X is the differentiation measure. PBS for population 1 was then estimated as:

$$\mathrm{PBS} = \frac{T_{12} + T_{13} - T_{23}}{2}$$

The obtained value quantifies the magnitude of allele frequency change in a lineage 1 since its divergence from the closely related population 2 and the outgroup 3. Lineage specific selection patterns among the focal populations were estimated by calculating PBS estimated for population trios J1-J3-GER and T1-T4-GER. The German population was chosen as the outgroup over the Swedish one, because it has a more equal genetic distance to each of our focal populations (Figure 1A and Table 1).

Outlier detection

We compared the PBS estimates against simulated samples to find sites that show higher differentiation than expected under neutrality. Neutral data were generated with coalescent models in ms (Hudson 2002), by taking into account the genome-wide recombination rates and the demographic history of these populations. This approach can produce realistic approximations of the null distribution, which generally leads to fewer false positives compared to methods based on specific population genetic or statistical models (Lotterhos and Whitlock 2015; Hoban et al. 2016). The relevant maximum likelihood estimates from the demography models (i.e. divergence times, migration rates and effective population sizes, going back to a most recent common ancestor of these populations) were used for each population comparison. Recombination rates for sequences that corresponded in size to observed window lengths were pulled randomly from a linkage map published in an earlier study (Hämälä et al. 2017). The mutation rate was set to 7×10^{-9} following Ossowski et al. (2010). Using the simulated data, we acquired ~50,000 neutral PBS estimates for each population, which constituted the null distributions for outlier testing. We defined *p*-values as the proportion of neutral estimates that had the same or higher PBS value than the observed one. To address the multiple testing issue, *p*-values were transformed into false discovery rate based *q*-values (Storey and Tibshirani 2003). We have implemented this PBS scan and outlier detection method into a new C program, PBScan, available at: https://github.com/thamala/PBScan

For one especially interesting locus, we also examined what evolutionary scenarios may have produced the selection patterns by conducting simulations under different forward genetic models in SLiM 2 (Haller and Messer 2017). As in the case of neutral simulations, we used the estimated demography parameters, mutation rate from Ossowski et al. (2010) and recombination information from Hämälä et al. (2017). Selection parameters (α [$2N_es$] = 10^2, 10^3, 10^4) were based on Pennings and Hermisson (2006). Code for the SLiM 2 simulations is available at: https://github.com/thamala/SLiM2_scripts

Gene Ontology enrichment analysis

Windows with significant (q-value < 0.05) outlier status were annotated with SnpEff (Cingolani et al. 2012) and genes that localized within or were closer than 5 Kb of an outlier window were included in a Gene Ontology (GO) (Ashburner et al. 2000) analysis. PANTHER tools (Mi et al. 2017) was used to detect significantly enriched terms (last accessed 19th of July 2017).

Acknowledgements

We thank H. Stenøien for sharing information about the *A. lyrata* growing sites in Norway, T. Toivainen and J. Tyrmi for sample collections and T. Mattila for providing part of the data set. We are also grateful for P. Ingvarsson and members of the Plant Genetics Group in Oulu for valuable discussions and comments on the manuscript. IT Center for Science (CSC) supplied computational resources. This work was supported by Biocenter Oulu (to T.H and O.S), Eemil Aaltonen Foundation (to T.H) and Academy of Finland's Research Council for Biosciences and Environment (decision 132611 to O.S).

References

Aeschbacher, S., J. P. Selby, J. H. Willis, and G. Coop. 2017. Population-genomic inference of the strength and timing of selection against gene flow. Proc. Natl. Acad. Sci. 114:7061–7066.

Anderson, J. T., C. R. Lee, C. A. Rushworth, R. I. Colautti, and T. Mitchell-Olds. 2013. Genetic trade-offs and conditional neutrality contribute to local adaptation. Mol. Ecol. 22:699–708.

Antonovics, J., and A. D. Bradshaw. 1970. Evolution in closely adjacent plant populations. VIII. Clinal patterns at a mine boundary. Heredity. 23:507–524.

Arnold, B. J., B. Lahner, J. M. DaCosta, C. M. Weisman, J. D. Hollister, D. E. Salt, K. Bomblies, and L. Yant. 2016. Borrowed alleles and convergence in serpentine adaptation. Proc. Natl. Acad. Sci. 113:8320–8325.

Ashburner, M., C. A. Ball, J. A. Blake, D. Botstein, H. Butler, J. M. Cherry, A. P. Davis, K. Dolinski, S. S. Dwight, J. T. Eppig, M. A. Harris, D. P. Hill, L. Issel-Tarver, A. Kasarskis, S. Lewis, J. C. Matese, J. E. Richardson, M. Ringwald, G. M. Rubin, and G. Sherlock. 2000. Gene Ontology: tool for the unification of biology. Nat. Genet. 25:25–29.

Bhatia, G., N. Patterson, S. Sankararaman, and A. L. Price. 2013. Estimating and interpreting F_{ST} The impact of rare variants. Genome Res. 23:1514–21.

Bolger, A. M., M. Lohse, and B. Usadel. 2014. Trimmomatic: A flexible trimmer for Illumina sequence data. Bioinformatics 30:2114–2120.

Charlesworth, B. 1998. Measures of divergence between populations and the effect of forces that

reduce variability. Mol. Biol. Evol. 15:538–543.

Chen, J., S. Glemin, and M. Lascoux. 2017. Genetic diversity and the efficacy of purifying selection across plant and animal species. Mol. Biol. Evol. 34:1417–1428.

Cingolani, P., A. Platts, L. L. Wang, M. Coon, T. Nguyen, L. Wang, S. J. Land, X. Lu, and D. M. Ruden. 2012. A program for annotating and predicting the effects of single nucleotide polymorphisms, SnpEff. Fly. 6:80–92.

Cruickshank, T. E., and M. W. Hahn. 2014. Reanalysis suggests that genomic islands of speciation are due to reduced diversity, not reduced gene flow. Mol. Ecol. 23:3133–3157.

DePristo, M. A., E. Banks, R. Poplin, K. V Garimella, J. R. Maguire, C. Hartl, A. A. Philippakis, G. del Angel, M. A. Rivas, M. Hanna, A. McKenna, T. J. Fennell, A. M. Kernytsky, A. Y. Sivachenko, K. Cibulskis, S. B. Gabriel, D. Altshuler, and M. J. Daly. 2011. A framework for variation discovery and genotyping using next-generation DNA sequencing data. Nat. Genet. 43:491–8.

Excoffier, L., I. Dupanloup, E. Huerta-Sánchez, V. C. Sousa, and M. Foll. 2013. Robust demographic inference from genomic and SNP data. PLoS Genet. 9:e1003905.

Farmer, L. M., A. J. Book, K.-H. Lee, Y.-L. Lin, H. Fu, and R. D. Vierstra. 2010. The RAD23 family provides an essential connection between the 26S proteasome and ubiquitylated proteins in *Arabidopsis*. Plant Cell 22:124–42.

Fischer, M. C., C. Rellstab, A. Tedder, S. Zoller, F. Gugerli, K. K. Shimizu, R. Holderegger, and A. Widmer. 2013. Population genomic footprints of selection and associations with climate in natural populations of *Arabidopsis halleri* from the Alps. Mol. Ecol. 22:5594–5607.

Fournier-Level, A., A. Korte, M. D. Cooper, M. Nordborg, J. Schmitt, and a. M. Wilczek. 2011. A map of local adaptation in *Arabidopsis thaliana*. Science. 334:86–89.

Gaudeul, M., H. K. Stenøien, and J. Ågren. 2007. Landscape structure, clonal propagation, and genetic diversity in Scandinavian populations of *Arabidopsis lyrata* (Brassicaceae). Am. J. Bot. 94:1146–1155.

Gonzalo-Turpin, H., and L. Hazard. 2009. Local adaptation occurs along altitudinal gradient despite the existence of gene flow in the alpine plant species *Festuca eskia*. J. Ecol. 97:742–751.

Griswold, C. K. 2006. Gene flow's effect on the genetic architecture of a local adaptation and its consequences for QTL analyses. Heredity. 96:445–453.

Gy, I., V. Gasciolli, D. Lauressergues, J.-B. Morel, J. Gombert, F. Proux, C. Proux, H. Vaucheret, and A. C. Mallory. 2007. *Arabidopsis* FIERY1, XRN2, and XRN3 are endogenous RNA silencing suppressors. Plant Cell 19:3451–61.

Günther, T., C. Lampei, I. Barilar, and K. J. Schmid. 2016. Genomic and phenotypic differentiation of *Arabidopsis thaliana* along altitudinal gradients in the North Italian Alps. Mol. Ecol. 25:3574–3592.

Haldane, J. B. S. 1930. A mathematical theory of natural and artificial selection. (Part VI, Isolation.). Math. Proc. Cambridge Philos. Soc. 26:220.

Haller, B. C., and P. W. Messer. 2017. SLiM 2: flexible, interactive forward genetic simulations. Mol. Biol. Evol. 34:230–240.

Hermisson, J., and P. S. Pennings. 2017. Soft sweeps and beyond: understanding the patterns and probabilities of selection footprints under rapid adaptation. Methods Ecol. Evol. 8:700–716.

Hoban, S., J. L. Kelley, K. E. Lotterhos, M. F. Antolin, G. Bradburd, D. B. Lowry, M. L. Poss, L. K.

Reed, A. Storfer, and M. C. Whitlock. 2016. Finding the genomic basis of local adaptation: pitfalls, practical solutions, and future directions. Am. Nat. 188:379–397.

Hohenlohe, P. A., S. Bassham, P. D. Etter, N. Stiffler, E. A. Johnson, and W. A. Cresko. 2010. Population genomics of parallel adaptation in threespine stickleback using sequenced RAD tags. PLoS Genet. 6:e1000862.

Hu, T. T., P. Pattyn, E. G. Bakker, J. Cao, J.-F. Cheng, R. M. Clark, N. Fahlgren, J. A. Fawcett, J. Grimwood, H. Gundlach, G. Haberer, J. D. Hollister, S. Ossowski, R. P. Ottilar, A. A. Salamov, K. Schneeberger, M. Spannagl, X. Wang, L. Yang, M. E. Nasrallah, J. Bergelson, J. C. Carrington, B. S. Gaut, J. Schmutz, K. F. X. Mayer, Y. Van De Peer, I. V Grigoriev, M. Nordborg, D. Weigel, and Y.-L. Guo. 2011. The *Arabidopsis lyrata* genome sequence and the basis of rapid genome size change. Nat. Genet. 43:476–483.

Hudson, R. R. 2002. Generating samples under a Wright-Fisher neutral model of genetic variation. Bioinformatics 18:337–338.

Hudson, R. R., M. Slatkin, and W. P. Maddison. 1992. Estimation of levels of gene flow from DNA sequence data. Genetics 132:583–589.

Hämälä, T., T. M. Mattila, P. H. Leinonen, H. Kuittinen, and O. Savolainen. 2017. Role of seed germination in adaptation and reproductive isolation in *Arabidopsis lyrata*. Mol. Ecol. 26:3484–3496.

Hämälä, T., T. M. Mattila, and O. Savolainen. 2018. Local adaptation and ecological differentiation under selection, migration and drift in *Arabidopsis lyrata*. Evolution. 72:1373–1386.

Kawecki, T. J., and D. Ebert. 2004. Conceptual issues in local adaptation. Ecol. Lett. 7:1225–1241.

Kim, S., K. E. Lohmueller, A. Albrechtsen, Y. Li, T. Korneliussen, G. Tian, N. Grarup, T. Jiang, G. Andersen, D. Witte, T. Jorgensen, T. Hansen, O. Pedersen, J. Wang, and R. Nielsen. 2011. Estimation of allele frequency and association mapping using next-generation sequencing data. BMC Bioinformatics 12:231.

Korneliussen, T. S., A. Albrechtsen, and R. Nielsen. 2014. ANGSD: Analysis of next generation sequencing data. BMC Bioinformatics 15:1471–2105.

Kubota, S., T. Iwasaki, K. Hanada, A. J. Nagano, A. Fujiyama, A. Toyoda, S. Sugano, Y. Suzuki, K. Hikosaka, M. Ito, and S. I. Morinaga. 2015. A genome scan for genes underlying microgeographic-scale local adaptation in a wild *Arabidopsis* species. PLoS Genet. 11:e1005361.

Körner, C. 2007. The use of "altitude" in ecological research. Trends Ecol. Evol. 22:569–574.

Latta, R. G. 1998. Differentiation of allelic frequencies at quantitative trait loci affecting locally adaptive traits. Am. Nat. 151:283–292.

Lenormand, T. 2002. Gene flow and the limits to natural selection. Trends Ecol. Evol. 17:183–189.

Lenormand, T., and S. P. Otto. 2000. The evolution of recombination in a heterogeneous environment. Genetics 156:423–438.

Lewontin, R. C., and J. Krakauer. 1973. Distribution of gene frequency as a test of the theory of the selective neutrality of polymorphisms. Genetics 74:175–195.

Li, H., and R. Durbin. 2009. Fast and accurate short read alignment with Burrows-Wheeler transform. Bioinformatics 25:1754–1760.

Li, J., T. M. Ou-Lee, R. Raba, R. G. Amundson, and R. L. Last. 1993. Arabidopsis flavonoid mutants are hypersensitive to UV-B irradiation. Plant Cell 5:171–179.

Lotterhos, K. E., and M. C. Whitlock. 2015. The relative power of genome scans to detect local adaptation depends on sampling design and statistical method. Mol. Ecol. 24:1031–1046.

Marques, D. A., K. Lucek, J. I. Meier, S. Mwaiko, C. E. Wagner, L. Excoffier, and O. Seehausen. 2016. Genomics of rapid incipient speciation in sympatric threespine stickleback. PLoS Genet. 12:e1005887.

Martin, G., and T. Lenormand. 2006. The fitness effect of mutations across environments: a survey in light of fitness landscape models. Evolution. 60:2413.

Mattila, T. M., J. Tyrmi, T. Pyhäjärvi, and O. Savolainen. 2017. Genome-wide analysis of colonization history and concomitant selection in *Arabidopsis lyrata*. Mol. Biol. Evol. 34:2665–2677.

Mi, H., X. Huang, A. Muruganujan, H. Tang, C. Mills, D. Kang, and P. D. Thomas. 2017. PANTHER version 11: Expanded annotation data from Gene Ontology and Reactome pathways, and data analysis tool enhancements. Nucleic Acids Res. 45:D183–D189.

Nei, M. 1986. Definition and estimation of fixation indexes. Evolution. 40:643–645.

Nei, M. 1987. Molecular evolutionary genetics. Columbia university press.

Nei, M., and W.-H. Li. 1979. Mathematical model for studying genetic variation in terms of restriction endonucleases. Proc. Natl. Acad. Sci. 76:5269–5273.

Nielsen, R., J. S. Paul, A. Albrechtsen, and Y. S. Song. 2011. Genotype and SNP calling from next-generation sequencing data. Nat. Rev. Genet. 12:443–451.

Ossowski, S., K. Schneeberger, and J. Lucas-Lledó. 2010. The rate and molecular spectrum of spontaneous mutations in *Arabidopsis thaliana*. Science. 327:92–94.

Pennings, P. S., and J. Hermisson. 2006. Soft sweeps II - Molecular population genetics of adaptation from recurrent mutation or migration. Mol. Biol. Evol. 23:1076–1084.

Pfeifer, S. P., S. Laurent, V. C. Sousa, C. R. Linnen, M. Foll, L. Excoffier, H. E. Hoekstra, and J. D. Jensen. 2018. The evolutionary history of Nebraska deer mice: Local adaptation in the face of strong gene flow. Mol. Biol. Evol. 35:792–806.

Price, N., B. T. Moyers, L. Lopez, J. R. Lasky, J. G. Monroe, J. L. Mullen, C. G. Oakley, J. Lin, J. Ågren, D. R. Schrider, A. D. Kern, and J. K. McKay. 2018. Combining population genomics and fitness QTLs to identify the genetics of local adaptation in *Arabidopsis thaliana*. Proc. Natl. Acad. Sci. 115:5028–5033.

Renaut, S., C. J. Grassa, S. Yeaman, B. T. Moyers, Z. Lai, N. C. Kane, J. E. Bowers, J. M. Burke, and L. H. Rieseberg. 2013. Genomic islands of divergence are not affected by geography of speciation in sunflowers. Nat. Commun. 4:1827.

Reynolds, J., B. S. Weir, and C. C. Cockerham. 1983. Estimation of the coancestry coefficient: Basis for a short-term genetic distance. Genetics 105:767–779.

Sambatti, J. B. M., and K. J. Rice. 2006. Local adaptation, patterns of selection, and gene flow in the Californian serpentine sunflower (*Helianthus exilis*). Evolution. 60:696–710.

Samuk, K., G. L. Owens, K. E. Delmore, S. E. Miller, D. J. Rennison, and D. Schluter. 2017. Gene flow and selection interact to promote adaptive divergence in regions of low recombination. Mol. Ecol. 26:4378–4390.

Savolainen, O., M. Lascoux, and J. Merilä. 2013. Ecological genomics of local adaptation. Nat. Rev. Genet. 14:807–820.

Schmitz, J., L. Heinrichs, F. Scossa, A. R. Fernie, M. L. Oelze, K. J. Dietz, M. Rothbart, B. Grimm, U. I. Flügge, and R. E. Häusler. 2014. The essential role of sugar metabolism in the acclimation response of *Arabidopsis thaliana* to high light intensities. J. Exp. Bot. 65:1619–1636.

Skotte, L., T. S. Korneliussen, and A. Albrechtsen. 2013. Estimating individual admixture proportions from next generation sequencing data. Genetics 195:693–702.

Slatkin, M. 1975. Gene flow and selection in a two-locus system. Genetics 81:787–802.

Storey, J. D., and R. Tibshirani. 2003. Statistical significance for genomewide studies. Proc. Natl. Acad. Sci. 100:9440–9445.

Tajima, F. 1989. Statistical method for testing the neutral mutation hypothesis by DNA polymorphism. Genetics 123:585–595.

Tiffin, P., and J. Ross-Ibarra. 2014. Advances and limits of using population genetics to understand local adaptation. Trends Ecol. Evol. 29:673–680.

Wadgymar, S. M., D. B. Lowry, B. A. Gould, C. N. Byron, R. M. Mactavish, and J. T. Anderson. 2017. Identifying targets and agents of selection: innovative methods to evaluate the processes that contribute to local adaptation. Methods Ecol. Evol. 8:738–749.

Wang, C., F. Gao, J. Wu, J. Dai, C. Wei, and Y. Li. 2010. Arabidopsis putative deacetylase AtSRT2 regulates basal defense by suppressing *PAD4*, *EDS5* and *SID2* expression. Plant Cell Physiol. 51:1291–1299.

Wang, J., J. Ding, B. Tan, K. M. Robinson, I. H. Michelson, A. Johansson, B. Nystedt, D. G. Scofield, O. Nilsson, S. Jansson, N. R. Street, and P. K. Ingvarsson. 2018. A major locus controls local adaptation and adaptive life history variation in a perennial plant. Genome Biol. 19:72.

Weir, B. S., and C. C. Cockerham. 1984. Estimating *F*-statistics for the analysis of population structure. Evolution. 38:1358–1370.

Weir, B. S., and W. G. Hill. 2002. Estimating *F*-statistics. Annu. Rev. Genet. 36:721–50.

Wright, S. 1931. Evolution in Mendelian populations. Genetics 16:97–159.

Yeaman, S., K. A. Hodgins, K. E. Lotterhos, H. Suren, S. Nadeau, J. C. Degner, K. A. Nurkowski, P. Smets, T. Wang, L. K. Gray, K. J. Liepe, A. Hamann, J. A. Holliday, M. C. Whitlock, L. H. Rieseberg, and S. N. Aitken. 2016. Convergent local adaptation to climate in distantly related conifers. Science. 353:23–26.

Yeaman, S., and M. C. Whitlock. 2011. The genetic architecture of adaptation under migration-selection balance. Evolution. 65:1897–1911.

Yi, X., Y. Liang, E. Huerta-Sanchez, X. Jin, Z. X. P. Cuo, J. E. Pool, X. Xu, H. Jiang, N. Vinckenbosch, T. S. Korneliussen, H. Zheng, T. Liu, W. He, K. Li, R. Luo, X. Nie, H. Wu, M. Zhao, H. Cao, J. Zou, Y. Shan, S. Li, Q. Yang, Asan, P. Ni, G. Tian, J. Xu, X. Liu, T. Jiang, R. Wu, G. Zhou, M. Tang, J. Qin, T. Wang, S. Feng, G. Li, Huasang, J. Luosang, W. Wang, F. Chen, Y. Wang, X. Zheng, Z. Li, Z. Bianba, G. Yang, X. Wang, S. Tang, G. Gao, Y. Chen, Z. Luo, L. Gusang, Z. Cao, Q. Zhang, W. Ouyang, X. Ren, H. Liang, H. Zheng, Y. Huang, J. Li, L. Bolund, K. Kristiansen, Y. Li, Y. Zhang, X. Zhang, R. Li, S. Li, H. Yang, R. Nielsen, J. Wang, and J. Wang. 2010. Sequencing of 50 human exomes reveals adaptation to high altitude. Science. 329:75–78.

Yoder, J. B., and P. Tiffin. 2017. Effects of gene action, marker density, and timing of selection on the performance of landscape genomic scans of local adaptation. J. Hered. 109:16–28.

Zakrzewska-Placzek, M., F. F. Souret, G. J. Sobczyk, P. J. Green, and J. Kufel. 2010. *Arabidopsis*

thaliana XRN2 is required for primary cleavage in the pre-ribosomal RNA. Nucleic Acids Res. 38:4487–4502.

Ågren, J., C. G. Oakley, J. K. McKay, J. T. Lovell, and D. W. Schemske. 2013. Genetic mapping of adaptation reveals fitness tradeoffs in *Arabidopsis thaliana*. Proc. Natl. Acad. Sci. 110:21077–21082.

Supplementary material

Table S1. The maximum likelihood functions (L) and Akaike information criterion (AIC) scores for each tested migration model. The best fitting models for each population comparison are in bold.

Population model	Migration model	$\log_{10}(L)$	AIC
J1-J3-GER	No migration	-812518.216	1625050
	From J1 to J3	-812517.500	1625051
	From J3 to J1	-812514.302	1625045
	Bidirectional migration	**-812473.580**	**1624965**
T1-T4-GER	No migration	-794034.865	1588084
	From T1 to T4	-794028.514	1588073
	From T4 to T1	-794017.947	1588052
	Bidirectional migration	**-794010.067**	**1588038**
J1-T1-GER	No migration	-819066.549	1638147
	From J1 to T1	**-819031.510**	**1638079**
	From T1 to J1	-819032.371	1638081
	Bidirectional migration	-819059.187	1638136
J3-T4-GER	**No migration**	**-864472.383**	**1728959**
	From J3 to T4	-864495.367	1729007
	From T4 to J3	-864488.217	1728992
	Bidirectional migration	-864519.009	1729056

Table S2. Maximum likelihood estimates (MLE) and their 95% confidence intervals for the demography parameters estimated with fastsimcoal2.

Parameter	MLE	95% CI
N_{J1}	3,370	2,691 – 4,988
N_{J3}	4,295	3,776 – 5,788
N_{T1}	1,862	1,049 – 2,481
N_{T4}	779	514 – 1,171
N_{GER}	51,351	43,854 – 61,369
$M_{J1\text{-}J3}$	0.266	0.077 – 1.503
$M_{J3\text{-}J1}$	9.748	6.033 – 10.918
$M_{T1\text{-}T4}$	0.034	0.002 – 1.021
$M_{T4\text{-}T1}$	0.083	0.007 – 2.491
$M_{J1\text{-}T1}$	0.004	0.001 – 0.322
$T_{J1\text{-}J3}$	866	637 – 1,097
$T_{T1\text{-}T4}$	307	214 – 602
$T_{JOT\text{-}TRO}$	1,393	1,022 – 1,725
$T_{GER\text{-}NOR}$	27,813	23,450 – 33,279

N is the effective diploid population size (N_e), M is the population migration rate $4N_em$, and T is the divergence time in number of generations. JOT-TRO indicates the divergence between Jotunheimen and Trollheimen and GER-NOR the divergence between Germany and Norway.

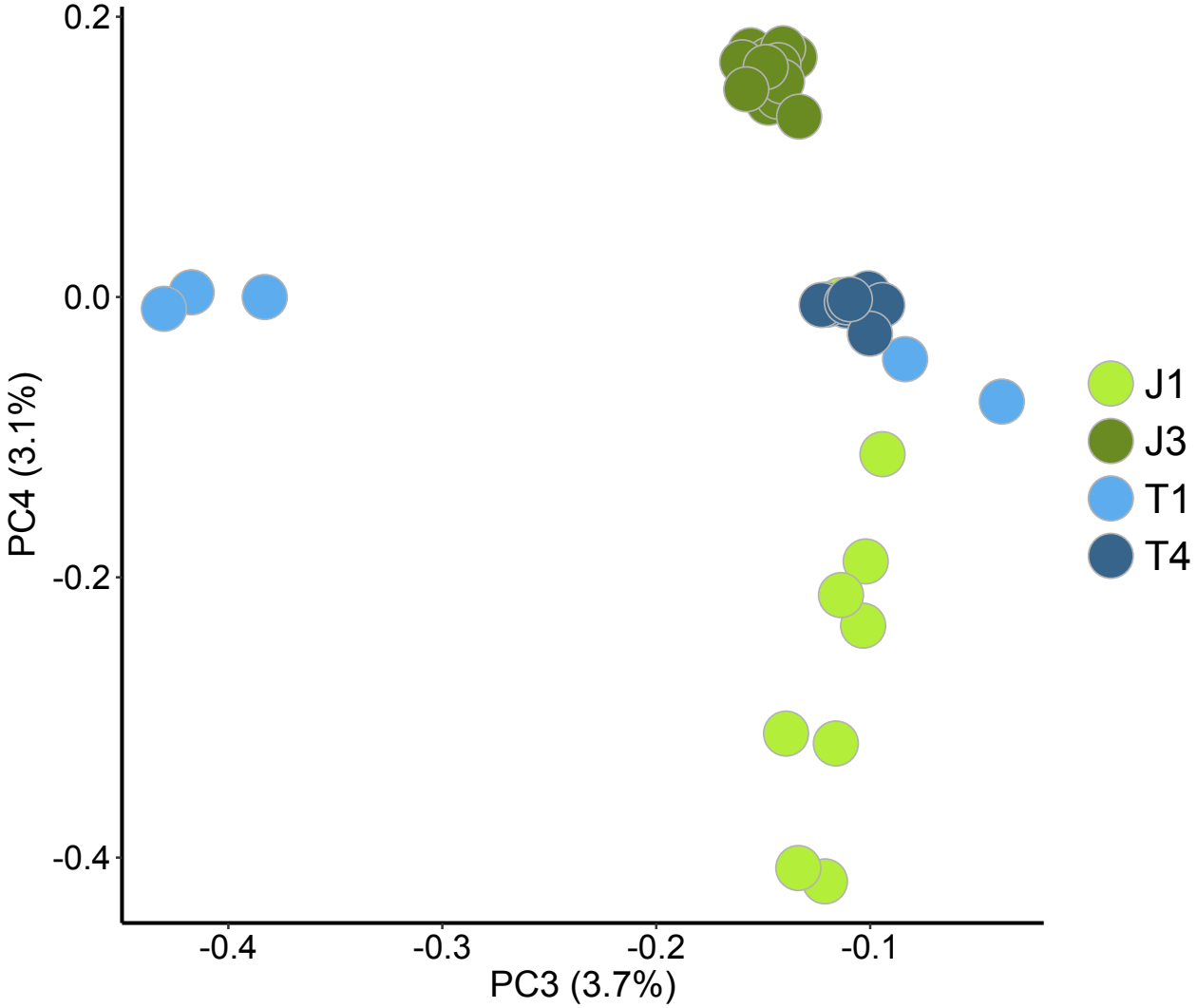

Figure S1. The third and the fourth principal components from the Norwegian-only PCA.

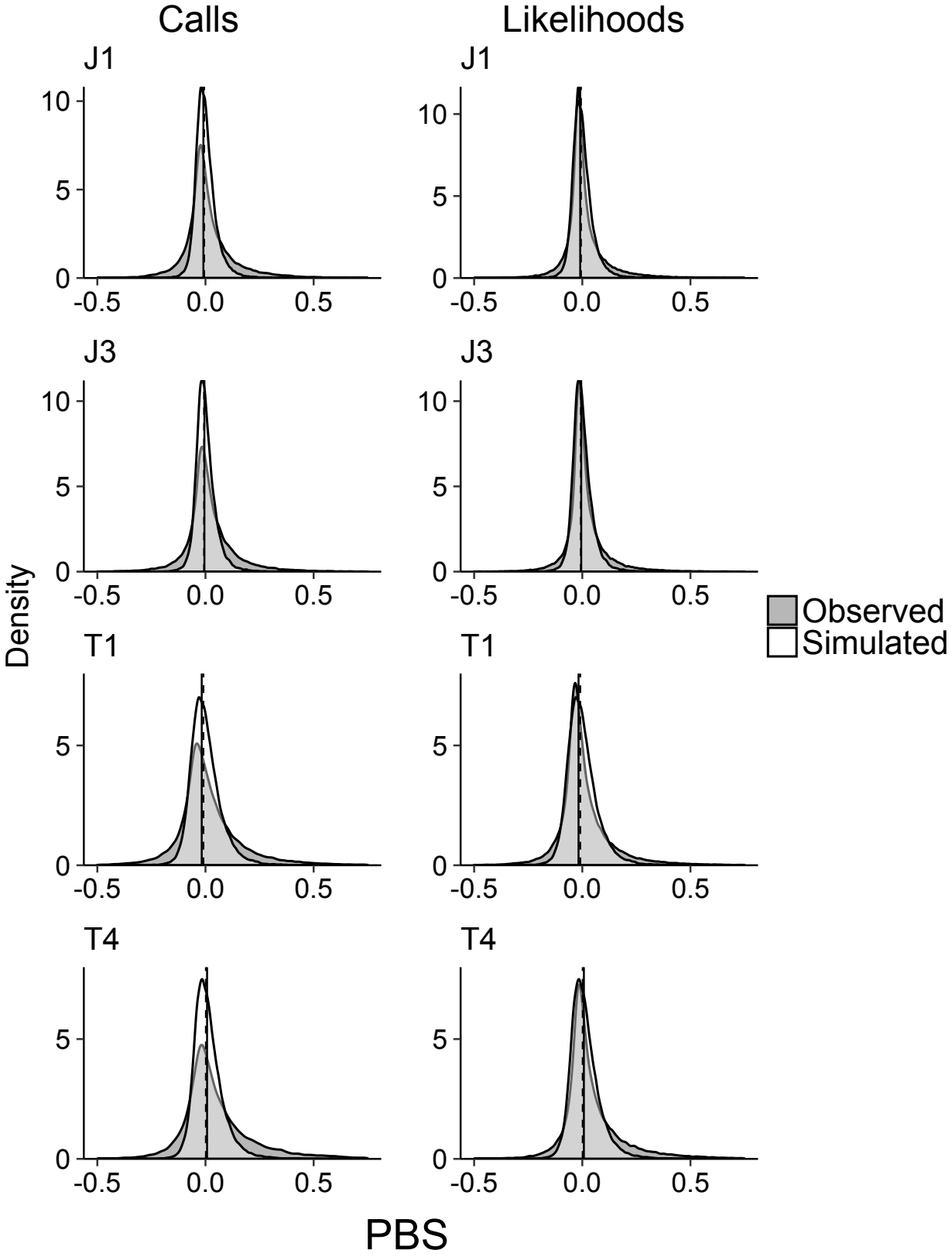

Figure S2. The PBS estimates generated with SNP calls and genotype likelihoods compared against simulated neutral samples. Data were filtered using the following settings: mapping quality 30, site quality 20, genotype quality 20 (SNP calls only), minimum coverage 4×. SNPs were called with Freebayes and the genotype likelihoods were estimated with the GATK model in ANGSD.

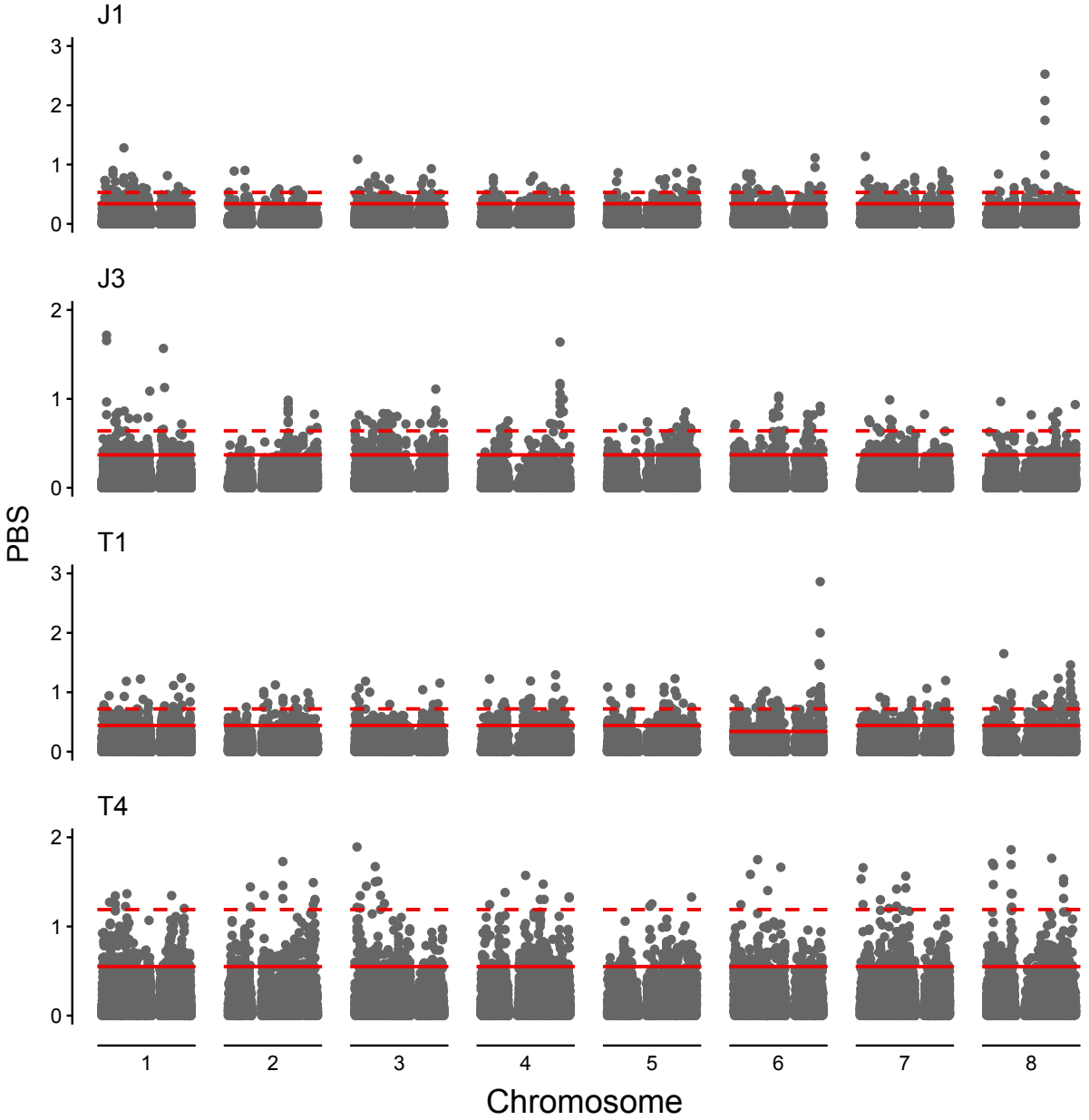

Figure S3. Population branch statistic (PBS) estimates along the genome. Solid red lines mark the *q*-value based significance thresholds at α = 0.05 level and dashed lines at α = 0.01 level.

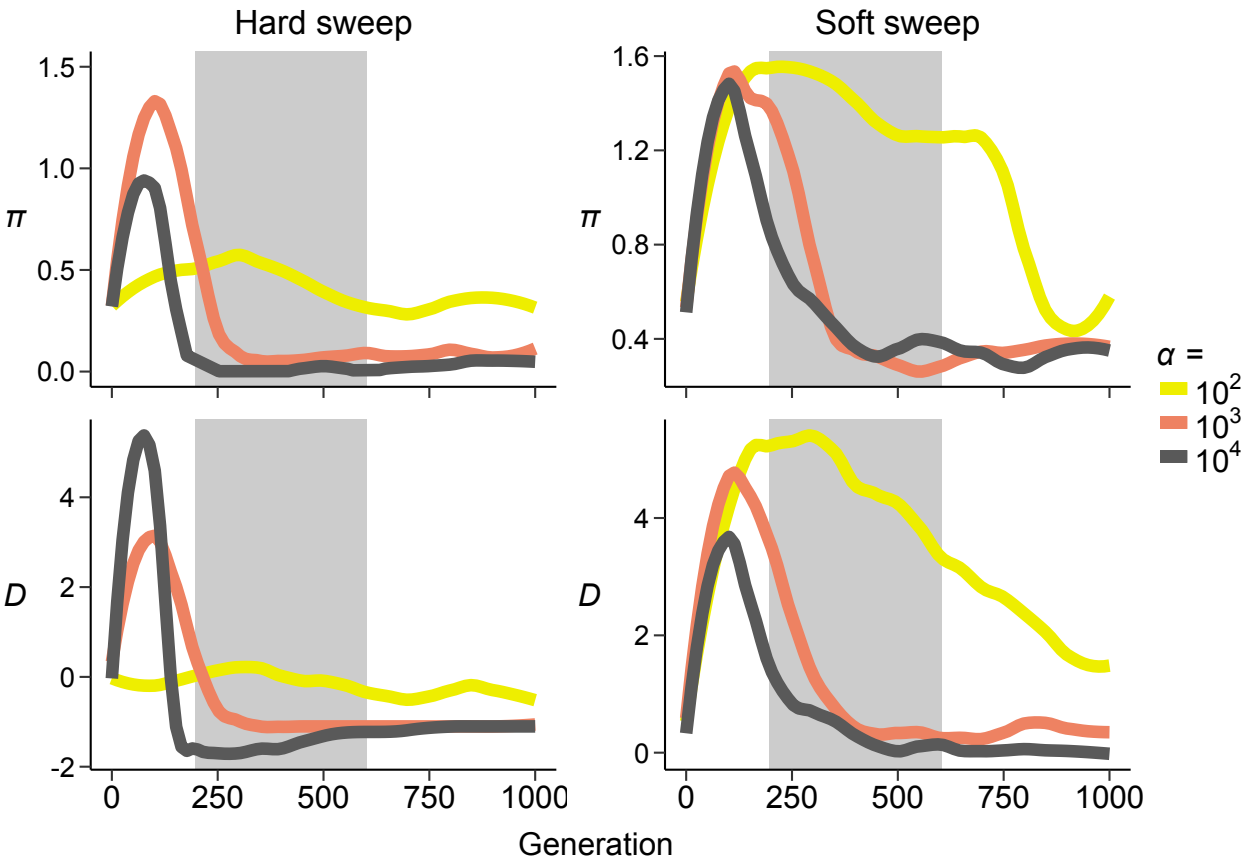

Figure S4. Nucleotide diversities and Tajima's *D*'s simulated with parameters: $2N_e = 1{,}558$ (corresponding to T4 estimate), α ($2N_es$) = 10^2, 10^3, 10^4, $\mu = 7\times10^{-9}$ and $r = 3.7\times10^{-8}$.